Increased number of islet-associated macrophages in type 2 diabetes

Ehses, J A ; Perren, A ; Eppler, E ; Ribaux, P ; Pospisilik, J A ; Maor-Cahn, R ; Gueripel, X ; Ellingsgaard, H ; Schneider, M K J ; Biollaz, G ; Fontana, A ; Reinecke, M ; Homo-Delarche, F ; Donath, M Y

Abstract: Activation of the innate immune system in obesity is a risk factor for the development of type 2 diabetes. The aim of the current study was to investigate the notion that increased numbers of macrophages exist in the islets of type 2 diabetes patients and that this may be explained by a dysregulation of islet-derived inflammatory factors. Increased islet-associated immune cells were observed in human type 2 diabetic patients, high-fat-fed C57BL/6J mice, the GK rat, and the db/db mouse. When cultured islets were exposed to a type 2 diabetic milieu or when islets were isolated from high-fat-fed mice, increased islet-derived inflammatory factors were produced and released, including interleukin (IL)-6, IL-8, chemokine KC, granulocyte colony-stimulating factor, and macrophage inflammatory protein 1alpha. The specificity of this response was investigated by direct comparison to nonislet pancreatic tissue and beta-cell lines and was not mimicked by the induction of islet cell death. Further, this inflammatory response was found to be biologically functional, as conditioned medium from human islets exposed to a type 2 diabetic milieu could induce increased migration of monocytes and neutrophils. This migration was blocked by IL-8 neutralization, and IL-8 was localized to the human pancreatic alpha-cell. Therefore, islet-derived inflammatory factors are regulated by a type 2 diabetic milieu and may contribute to the macrophage infiltration of pancreatic islets that we observe in type 2 diabetes.

DOI: https://doi.org/10.2337/db06-1650

Increased number of islet associated macrophages in type 2 diabetes

Received for publication 26 November 2006 and accepted in revised form 21 May 2007.

J. A. Ehses[1], A. Perren[2], E. Eppler[5], P. Ribaux[6], J. A. Pospisilik[7], R. Maor-Cahn[1], X. Gueripel[2], H. Ellingsgaard[1], M. K. J. Schneider[3], G. Biollaz[4], A. Fontana[4], M. Reinecke[5], F. Homo-Delarche[8], and M. Y. Donath[1#]

[1]Division of Endocrinology and Diabetes, and the Center for Integrated Human Physiology, [2]Department of Pathology, [3]Laboratory for Transplantation Immunology, [4]Division of Clinical Immunology, University Hospital of Zürich, 8045 Zürich, Switzerland.
[5]Division of Neuroendocrinology, Institute of Anatomy, University of Zurich, CH 8057, Zürich, Switzerland.
[6]Department of Medicine Genetic and Development, University Medical Center, Geneva, Switzerland.
[7]Institute of Molecular Biotechnology of the Austrian Academy of Science, Dr. Bohrgasse 3, 1030 Vienna, Austria.
[8]Unité mixte de recherches (UMR) 7059, National Center for Scientific Research (CNRS), Paris 7 University/D. Diderot, Paris, France.

#Address correspondence to:

Dr. J. A. Ehses
University Hospital of Zürich
Div. of Endocrinology & Diabetes
Rämistrasse 100
Zürich 8091
Switzerland
Email: jan.ehses@usz.ch

Dr. Marc Y. Donath
University Hospital of Zürich
Div. of Endocrinology & Diabetes
Rämistrasse 100
Zürich 8091
Switzerland
Email: marc.donath@usz.ch

Manuscript information: 31 text pages, 7 figures, 1 table.
Word count: Abstract 220 words, main text 4800 words.
Running title: Increased islet macrophages in type 2 diabetes.

ABSTRACT

Activation of the innate immune system in obesity is a risk factor for the development of type 2 diabetes. The aim of the current study was to investigate the notion that increased numbers of macrophages exist in the islets of type 2 diabetes patients, and that this may be explained by a dysregulation of islet-derived inflammatory factors. Increased islet-associated immune cells were observed in human type 2 diabetic patients, high fat (HF) fed C57BL/6 mice, the GK rat, and the db/db mouse. When cultured islets were exposed to a type 2 diabetic milieu or when islets were isolated from HF fed mice, increased islet-derived inflammatory factors were produced and released, including IL-6, IL-8, chemokine KC, G-CSF, and MIP-1α. The specificity of this response was investigated by direct comparison to non-islet pancreatic tissue and β-cell lines, and was not mimicked by the induction of islet cell death. Further, this inflammatory response was found to be biologically functional, since conditioned medium from human islets exposed to a type 2 diabetic milieu could induce increased migration of monocytes and neutrophils. This migration was blocked by IL-8 neutralization, and IL-8 was localized to the human pancreatic α-cell. Therefore, islet-derived inflammatory factors are regulated by a type 2 diabetic milieu and may contribute to the macrophage infiltration of pancreatic islets we observe in type 2 diabetes.

INTRODUCTION

Activation of the innate immune system has long been reported in obesity, insulin resistance, and type 2 diabetics, characterized by increased circulating levels of acute-phase proteins, and cytokines and chemokines (1-5). However, the notion that excess circulating nutrients may stimulate the β-cell to produce chemokines remains unexplored, and immune cell infiltration has not been shown in islets of type 2 diabetic patients.

One of the most classical chemotactic agents in immunology is the CXC family chemokine, IL-8 (CXCL8)(6). IL-8 is produced by leukocytes, fibroblasts, endothelial and epithelial cells, and is commonly associated with infections, graft rejection, allergy, asthma, cancer, and atherosclerosis. In addition to its effect on neutrophils, the chemotactic effect of IL-8 is also important in mediating monocyte migration (7-9). The rodent does not express IL-8. Instead, the rodent functional homologue of IL-8 is thought to be chemokine KC (CXCL1, or Gro-α in the rat), which has also been reported to induce granulocyte and monocyte migration (9). Chemokine KC is thought to be an ortholog of human CXCL1. Circulating levels of IL-8 are elevated in type 2 diabetics (10; 11), where it has been implicated in systemic insulin resistance and atherosclerosis (12; 13).

Thus, we hypothesized that pancreatic islets in type 2 diabetes are characterized by increased macrophage infiltration, and that a type 2 diabetic milieu could promote chemokine production in pancreatic islets. In investigating this premise, we found increased numbers of macrophages associated with islets of type 2 diabetes patients and animal models of this disease, and have identified various nutrient-regulated islet-derived inflammatory factors (including IL-6, IL-8, chemokine KC, G-CSF, and MIP-1α). Given these factors, we have identified IL-8 to be an integral chemokine mediating monocyte and neutrophil chemotaxis by conditioned medium from human islets exposed to a type 2 diabetic milieu. Finally, we have localized islet-derived IL-8 to the human pancreatic α-cell.

RESEARCH DESIGN AND METHODS

Tissue samples and immunohistochemistry. For specific human sample information, see Table 1. Patients with pancreatitis, lymphoma, systemic infection, and on immunosuppressive therapy were excluded from analysis. Pancreata were procured for histology and islet isolation according to regulations and good practice rules applied at that time in Switzerland. Briefly, consent was considered obtained if the potential donor carried an official organ Swisstransplant (Swiss national organ sharing agency) donor card, on which individual reservations about procurement of specific organs or tissues are explicitly mentioned. For brain-dead potential donors not carrying an organ donor card, consent was obtained orally from the closest relatives and specifically mentioning the use of the pancreas for islet

isolation or histology. Use of pancreatic tissue was approved by the cantonal ethical committee, number StV 29-2006.

Immune cell immunohistochemistry: Human tissue samples were fixed in formalin, 4 μm sections were cut, and immunohistochemistry was performed on an automated stainer (Ventana benchmark, Tucson, AZ, USA) after protease 1 (Ventana) pretreatment. Sections were incubated with an anti-CD68, anti-CD163, or anti-HLA 2 antibody (Ab; mouse anti-human CD68, clone PG-M1, 1:50, Dako, Glostrup, Denmark; mouse anti-human CD163, clone 163C01/10D6, 1:100, NeoMarkers/Lab Vision Corporation, Newmarket Suffolk, UK; mouse anti-human HLA Class 2 (DP+DQ+DR), clone IQU9, 1:50, Novocastra Laboratories Ltd, Newcastle, UK), followed by a biotinylated secondary Ab (Ventana). Staining was visualized with the I-view DAB detection kit (Ventana). Sections were co-stained with an anti-insulin Ab (polyclonal guinea pig anti-insulin, 1:500, Dako) followed by a prediluted secondary Ab, and chromogenically detected via the Ventana alkaline phosphatase (AP) Fast Red Kit. Counterstaining was done with hematoxylin. Islet associated granulocytes were stained for by H&E morphology and using an anti-human myeloperoxidase Ab (Rabbit polyclonal, 1:15000; Dako). The CD68 Ab was used as previously shown (14), and controlled by mouse IgG Ab staining. For TUNEL detection, sections were permeabilized with proteinase K (20 μg/mL) and endogenous peroxidases were blocked with 3 % H2O2. Sections were incubated with working strength TdT enzyme (ApopTag kit S7100; Millipore; Switzerland). After rinsing sections with a stop-buffer the slides were covered by anti-digoxigenin peroxidase conjugate, rinsed and then incubated with rabbit anti-sheep HRP antibody (1:80). Detection was performed with DAB (Ventana) and haematoxylin was used for counterstaining.

Mouse pancreatic cryosections were incubated with an anti-Cd11b primary Ab (BD Pharmingen, Basel, Switzerland; 1:167), isotype rat IgG2B (Serotec, Düsseldorf, Germany), anti-insulin Ab (Dako), and Dapi to identify nuclei. This Cd11b Ab has been published by us previously (15); mouse spleen served as a positive tissue control. Primary Abs were visualized using Strep-Cy3 secondary and FITC secondary antibodies respectively (Jackson Immunoresearch, Newmarket, UK), and pictures captured on an Axioplan2 imaging system (Zeiss, Feldbach, Switzerland). Additionally, some sections were visualized with 3-amino-9-ethylcarbazole (AEC) substrate and counterstained with hematoxylin.

Wistar and GK rat cryosections were incubated with mouse anti-rat-IA (MHC II; Serotec; 1:300) and ED1 mouse anti-rat CD68 (Serotec; 1:100), followed by incubation with goat anti-mouse secondary (Caltag, Cergy, France) and visualized with AEC substrate. For each series of pancreas sections, one slide was stained only with the second antibody as a control for endogenous peroxidase activity and non-specific antibody binding as previously published (16).

IL-8 immunohistochemistry: Pancreatic resection samples (3 control and 4 type 2 diabetic patients) and sorted human non-beta cells plated on ECM were analyzed for IL-8 expression. Human glioblastoma sections were used as a positive control for IL-8 staining as previously shown (17). Sections and sorted non-beta cells were incubated with a rabbit anti-IL-8 primary Ab (Abcam ab16223, Cambridge, UK; 1:50), or isotype control (rabbit IgG, R&D Systems, Abingdon, UK). Antibody specificity was tested using recombinant IL-8 protein (Abcam ab6931) to block binding. IL-8 was visualized using AEC, Cy-3 anti-rabbit, or Alexa Fluor®488 donkey anti-rabbit IgG secondary (Molecular probes, Eugene, OR, USA). Sections were further incubated with guinea pig anti-insulin or guinea pig anti-glucagon (Dako, 1:50) followed by a FITC secondary. Non-beta cells were incubated with the above glucagon Ab, rhodamine-conjugated goat anti-guinea pig (Jackson, Suffolk, UK) secondary, and nuclei were labeled with Hoechst 33342 (Sigma, Buchs, Switzerland). Further, the same IL-8 Ab was used in Western blotting of human islet samples. Recombinant IL-8 (R&D Systems) was used as a positive control for Western blotting.

Islet immune cell scoring: An average of 43 ± 17 islets from nondiabetic (n=7) and 35 ± 12 islets from diabetic (n=9) pancreatic sections were blindly scored for CD68+ cells around the periphery and/or within islets by two investigators (A.P and X.G). CD163 and HLA-2 was used to confirm macrophage identity in resection samples. To evaluate TUNEL+ cells localized to CD68+ infiltrated islets, 190 islets from 3 diabetic patients (resection samples) showing strong infiltration were evaluated in serial sections stained for TUNEL and CD68. Post-mortem interval time for autopsy samples ranged from 7-24h, and archive time for all samples ranged from 24-99 months. Pancreatic sections from the corpus and tail of the pancreas were examined.

Islet-associated Cd11b positive cells were scored by a single investigator (J.A.E.) blinded to the conditions. Only Cd11b positive cells around the periphery of pancreatic islets or within islets were scored. For each animal in the study (n=3-7), 4 to 8 pancreatic sections cut at 60-80 μm intervals were scored. Data are expressed as Cd11b positive cells/islet, where "islet" refers to a cross-sectionally detected islet defined by size (small islet: 1-5 cross sectional cells, medium islet: 5-20 cross sectional cells; large islet: 20-50 cross sectional cells). A total of 100 to 200 islets per treatment group were scored. Islet area was measured by assessing the area of insulin immunopositive cells, traced manually and computed using analySIS™ 3.1 software (Soft Imaging System GmbH, Münster, Germany). TUNEL positive cells were analyzed in 20.6 ± 0.4 islets and 25.0 ± 5.2 islets/animal in 8 and 16 week chow and HF fed animals (8 week; n=5 and 16 week: n=6; In Situ Cell Detection Kit, AP, Roche, Basel, Switzerland). Islet associated CD68+ and MHC II+ cells in Wistar and GK rats were scored in islets from 6 to 9 different animals.

Animals and glucose tolerance testing. Male C57BL/6J mice (Harlan, Horst, Netherlands) were used for all mouse islet experiments. In some cases, animals were fed a hypercaloric diet (high fat; HF) manufactured by Research Diets (New Brunswick, NJ, USA). The HF diet contained 58, 26 and 16% calories from fat, carbohydrate and protein, respectively, and a total of 5.6 kcal/g, whereas the control diet was manufactured by Provimi Kliba AG (Kaiseraugst, Switzerland) and contained 29, 39 and 32% calories from fat, carbohydrate and protein, respectively, and a total of 2.8 kcal/g. For assessment of Cd11b+ cells around islets, animals were started on HF diet at age 3-4 weeks, for *ex vivo* determination of islet cytokines and chemokines animals were started on HF diet at age 8 weeks. For glucose tolerance testing, mice were injected i.p. with 2 mg/g body weight glucose (IPGTT) and blood glucose concentration was measured with a Freestyle™ glucometer (Abbott, Baar, Switzerland).

Characteristics of the GK rat maintained in the colony at the Paris 7 University have been described previously (18). This animal model was developed by inbreeding Wistar rats with mild hyperglycemia. Male GK rats are normoglycemic prior to weaning (1 month), with hyperglycemia, hypercholesterolemia and hypertriglyceridemia developing shortly after weaning, followed by insulin resistance at 2 months. Male db/db and db/+ littermate controls were purchased from Jackson (Bar Harbour, ME, USA). Guidelines for the use and care of laboratory animals at the University of Zurich were followed.

Islet isolation, α-cell purification, and cell culture. Human islets were isolated from pancreata of 14 organ donors at the University of Geneva Medical Center and the University of Illinois at Chicago. All human islet preparations were stained with dithizone (>80% purity of islets) and insulin (40-50% β-cells/islet) to monitor purity, and were hand-picked and plated by a single investigator (J.A.E.) to maintain consistency. Human non-beta cells were isolated using a method adapted from (19) and (20) (Parnaud et al, submitted). Mouse islets and non-endocrine pancreatic tissue were isolated from C57BL/6J mice by collagenase digestion and hand-picking of islets. After collagenase digestion, non-endocrine tissue was recovered as a pellet and islets were removed by handpicking as reported (21). Human islets were cultured in CMRL 1066 medium containing 5.5 mM glucose, 100 U/mL penicillin, 100 ug/ml streptomycin, and 10 % FCS (Invitrogen Ltd., Basel, Switzerland). Mouse islets and non-endocrine tissue were cultured in RPMI 1640 medium containing 11 mM glucose, 100 U/ml penicillin, 100 μg/ml streptomycin, 40 μg/ml Gentamycin and 10% FCS (hereafter referred to as islet media). Islets were cultured on extracellular matrix (ECM)-coated plates (at 20 islets/plate) derived from bovine corneal endothelial cells (Novamed, Jerusalem, Israel) as previously described (22). In experiments using ECM dishes, islets and non-endocrine tissue were left 48 h in islet media to adhere and spread before initiation of experiments. INS-1 cells were kindly donated by Dr. S.A. Hinke (Belgium) and MIN-6 cells were donated by Dr.

P. Halban (Geneva), and cultured as previously described (23). MIN-6 and INS-1 cells were seeded at 5 x 10^5 cells/well and control conditions included 25 mM and 11 mM glucose media respectively.

In some experiments islets were treated with 33 mM glucose and/or 0.5 mM palmitate (Sigma). Palmitic acid was dissolved at 10 mmol/l in RPMI-1640 medium containing 11% fatty acid—free BSA (Sigma) under an N_2-atmosphere, shaken overnight at 55°C, sonicated 15 min, and filtrated under sterile conditions. For control incubations, 11% BSA was prepared, as described above. Before use, the effective free fatty acid concentrations were controlled with a commercially available kit (Wako, Neuss, Germany). In some experiments 500 nM staurosporine or 0.1 and 1 mM streptozotocin were added to mouse islets for 48h to induce cell death. Cell death was confirmed by TUNEL (Roche).

Insulin secretion. For acute insulin release in response to glucose, islets were washed and incubated in Krebs-Ringer buffer (KRB) containing 2.8 mM or 16.7 mM glucose and 0.5% BSA for 1 h. Islet insulin was extracted with 0.18 M HCl in 70% ethanol for determination of insulin content. Secreted insulin and insulin content was assayed by RIA (CIS Biointernational, Gif-sur-Yvette, France).

Cytokines and chemokines. Conditioned media and serum cytokines and chemokines were assayed using human, mouse, and rat Luminex™ kits. In some islet experiments cytokine/chemokine release was normalised to total islet protein, extracted using lysis buffer and measured using the BCA assay (Pierce, Rockford, IL, USA).

RNA extraction and real-time PCR. Total mouse islet RNA was extracted as described (22) and reverse transcribed using random hexamers. Commercially available mouse primers to 18S rRNA, IL-6, chemokine KC, G-CSF, and MIP-1α were purchased and assayed according to the manufacturer's protocol using the ABI 7000 system (Applied Biosystems, Foster City, CA, USA). Changes in mRNA expression were calculated using difference of C_T values.

Migration assay. To evaluate monocyte and neutrophil migration peripheral blood mononuclear cells (PBMCs) and granulocytes were isolated from a single healthy male donor using Histopaque®, as per the manufacturer's protocol (Sigma). Migration was tested using Transwell membranes by loading a mix of

1 x 10^6 PBMCs and 5 x 10^5 granulocytes into the upper chamber, and human islet medium or human islet supernatant into the lower chamber. Experiments were carried out in X-Vivo 15 medium (Cambrex, Verviers, Belgium), where islet culture medium and islet supernatants were diluted 10x. Human islet supernatants treated without (untreated) and with 33 mM glucose and 0.5 mM palmitate (treated) for 48h were used. Migration was allowed to proceed for 4 h at 37 ^oC before evaluation of total cells migrated by flow cytometry (FACScan,

BD Biosciences). Identification of migrated monocytes and neutrophils was achieved using FITC-conjugated anti-CD14 and CD15 monoclonal antibodies respectively (BD Biosciences). Appropriate isotype controls were used to ensure Ab specificity. IL-8 was neutralized by addition of an IL-8 antibody or normal goat isotype control (30 µg/mL; R&D Systems) to the lower chamber and preincubation for 30 minutes with conditioned media before the addition of cells to the upper chamber. In control experiments, the IL-8 antibody was found to block recombinant IL-8 induced migration.

IL-8 electron microscopy. Islets from 4 separate human islet isolations were fixed by immersion in a fixation solution containing 2,5% paraformaldehyde, 0,1% glutaraldehyde and 0,01% picric acid for 4 h. Thereafter, specimens were dehydrated and embedded routinely in LR White (Polysciences, Warrington, USA). Ultrathin sections were cut at 90 nm and transferred onto nickel grids (mesh size 100). Sections were incubated with a mouse glucagon antiserum (G-2654, Sigma, St. Louis, USA; 1:100) followed by biotinylated anti-mouse IgG (Amersham International, Dübendorf, Switzerland) and a streptavidin-gold-5 nm complex (Amersham). IL-8 was visualized using rabbit IL-8 antiserum (Abcam; 1:50) followed by biotinylated goat anti-rabbit IgG (Bioscience, Emmenbrücke, Switzerland) and a streptavidin-gold-15 nm complex (Amersham). Sections were examined with a Philips CM 100 electron microscope and digitally analysed with Gatan Bioscan Digital Micrograph (Gatan, Pleasanton, CA, USA).

Statistics. Data are expressed as means ± S.E. with the number of individual experiments presented in the figure legends. All data were tested for normality and analyzed using the nonlinear regression analysis program PRISM (GraphPad, CA, USA). Significance was tested using the Student's *t*-test and analysis of variance (ANOVA) with Bonferonni's or Dunnett's post hoc test for multiple comparison analysis. Significance was set at $p < 0.05$.

RESULTS

Increased number of pancreatic-islet associated macrophages in type 2 diabetes. We investigated whether type 2 diabetic islets display immune cell infiltration. With respect to human samples, we observed increased numbers of islet-associated macrophages (based on CD68, CD163, and HLA-2 immunolabeling; CD163 and HLA-2 not shown) in human type 2 diabetic tissue from both autopsy and resection samples (Table 1 and Figure 1A-B). Islets with increased numbers of macrophages (>3 CD68+ cells/islet) were observed more frequently in type 2 diabetic samples compared to non-diabetic controls (Figure 1A; maximum of 19 CD68+ cells/islet in type 2 diabetic samples). In contrast to islets of control patients with exclusive perivascular location of CD68+ macrophages, the affected islets showed intra-islet invasion (Figure 1B). Type 2 diabetic islets characterized by increased CD68+ cells did not display increased

TUNEL+ cells and we never observed macrophages in the vicinity of apoptotic β-cells (Figure 1B). Numbers of TUNEL+ cells were 0.023 ± 0.011 vs. 0.046 ± 0.004 TUNEL+ cells/islet for non-diabetic (n=4) vs. diabetic (n=3) resection samples analyzed respectively. Numbers of CD68+ cells/islet did not correlate with post-mortem interval of autopsy samples (r^2=0.15, p=0.34, n=8), or tissue archive time (r^2=0.00066, p=0.93, n=15). Cases with intra-islet invasion were associated with decreased insulin immuno-reactivity, and amyloid deposits. These macrophages were positive for HLA-2 and CD163 (data not shown). We saw no differences in pancreatic islet or exocrine associated granulocytes or CD3 positive T-cells in diabetic vs. non-diabetic samples, while some CD3 T-cells were observed in the peri-islet region of all samples.

To investigate the onset of increased islet-associated immune cells, we fed C57BL/6J mice a normal chow or HF diet and evaluated islet-associated CD11b+ cells (a marker for macrophages in addition to dendritic and other myeloid cell lineages) after 4, 8, and 16 weeks. After 8 weeks of HF feeding mice displayed glucose intolerance and remained so until the experiment was terminated at 16 weeks (Figure 1C). In this model Cd11b+ cells were observed mostly at the periphery of islets (Figure 1D); the spleen served as a positive control for Cd11b staining (Figure 1E). Already after 8 weeks of HF feeding, we detected a doubling in the number of islet-associated CD11b+ cells exclusively around large islets in HF fed animals vs. chow controls of the same age. At 16 weeks there was a trend towards increased CD11b+ cells around medium sized islets as well. Large islets with >3 CD11b+ cells were observed more frequently in HF sections compared to chow controls (10 ± 6 % (n=4) vs. 48 ± 15 % of total islets with >3 CD11b+ cells (n=5) in 8 week chow and HF fed samples respectively; p<0.05). Islet area of those large islets evaluated at 8 weeks was not significantly different in HF versus normal diet fed animals (28720 ± 8930, n=4 vs. 27440 ± 4210 μm^2; n=5). Thus, increased islet-associated CD11b+ cells around large islets was not due to a difference in islet size between normal and HF fed animals, and was detected as an early event following HF feeding. Analysis of islets in 8 and 16 week chow, and 8 week HF fed animals revealed no TUNEL positive cells. In 16 week HF fed animals, 0.031 TUNEL+ cells/islet (2 TUNEL+ cells/65 islets analyzed from n=3 animals with highest number of Cd11b+ cells/islet) were detected.

The GK rat is a rodent model of spontaneous type 2 diabetes established by inbreeding Wistar rats selected from the upper limit of a normal distribution for glucose tolerance (18). We analyzed the presence of islet-associated macrophages in 1-month (weaning; normogylcemic) and 2-month old male Wistar and GK rats (one month after chronic mild hyperglycemia; fasting glycemia: 6.3 ± 0.2 vs. 11.3 ± 0.6 mM, n=10 for Wistar and GK rats respectively; p<0.05) using 2 different antibodies, ED-1 (CD68) and anti-MHC class 2. There was no difference in macrophages associated with islets at 1 month of age (not shown). While few macrophages were present around Wistar islets, GK islets were

characterized by pronounced macrophage infiltration at 2 months of age (Figure 2). The mean islet area analyzed for CD68+ and MHC-2+ cells was identical in both strains for these comparisons (Figure 2B and D). Finally, we investigated 8-9 week old db/db mice and littermates (glucose intolerance develops between 4-8 weeks of age) for islet-associated Cd11b+ cells. Fasting glycemia was 4.0 $\pm$ 0.2 vs. 8.3 $\pm$ 0.7 mM for db/+ and db/db mice respectively (n=10, $p<0.05$). Compared to db/+ littermates, db/db mouse islets were characterized by increased peri-islet CD11b+ cell infiltration (2.6 $\pm$ 1.7 % (n=4) vs. 24.8 $\pm$ 4.9 % of total islets with >3 CD11b+ cells (n=5; $p<0.05$); 1.6 $\pm$ 0.1 vs. 2.4 $\pm$ 0.3 $Cd11b^+$ cells/islet; $p<0.05$, n=5 for db/+ and db/db respectively).

Human and mouse islets release increased amounts of cytokines and chemokines in response to a type 2 diabetic milieu. We hypothesized that pancreatic islets secrete factors that may attract macrophages under pathological conditions. After screening human islet, mouse islet and cell line preparations we concentrated on the regulation of IL-6, IL-8, G-CSF, IP-10, MIP-1α, MCP-1, and chemokine KC in the rodent (all known to be elevated in type 2 diabetic and obese subjects (1; 2; 24)). After 48 h of treatment with 33 mM glucose, or 0.5 mM palmitate (in combination or separately), we evaluated glucose-stimulated insulin secretion to ensure β-cell dysfunction (Figure 3A, B). As seen in Figure 3 (C-E), mouse and human islets released profoundly more IL-6, IL-8, chemokine KC and G-CSF in response to elevated glucose and palmitate in combination after 48 h of treatment, while palmitate alone stimulated only some of these factors. Note that rodents do not express IL-8, and chemokine KC is thought to be its functional homologue in rodents. Further, IP-10 showed a trend towards regulation in human islets, with no change in mouse islets (Figure 3F). MIP-1α release was also significantly increased in human islet preparations in response to a diabetic milieu (Figure 3G), but was undetectable in mouse islet supernatants (data not shown). Finally, MCP-1 remained unaffected in human islets (Figure 3H; undetectable in mouse islets).

The specificity of this islet inflammatory response to elevated glucose and palmitate was tested by comparison of endocrine and non-endocrine tissue, by analysis of β-cell lines, and by the induction of cell death. While gluco-lipotoxic stress increased IL-6, KC, and G-CSF release from islets, these factors were not significantly increased in an equal quantity of non-endocrine tissue (Figure 4A-D). Further, to support our claim that these factors are islet-cell derived, both MIN-6 cells and INS-1 cells were found to respond to elevated glucose and palmitate by releasing increased amounts of chemokine KC, G-CSF and MIP-1α (Figure 4E-H). Finally, to rule out that an unspecific stimulation by the apoptotic/necrotic process induced by glucose and palmitate was responsible for the increase in cytokine/chemokine release, we tested the effect of 48 h staurosporine (500 nM), and 0.1 and 1 mM streptozotocin treatment on mouse islets. Islet cell death induced by

either agent did not increase cytokine/chemokine release (Figure 4I-K).

To examine whether the nutrient effects on the above cytokine/chemokines are mediated at the transcriptional level, we isolated mouse islet RNA after 48 h treatment under gluco-lipotoxic conditions. In contrast to the response seen at the protein level, the IL-6 transcript was downregulated by a diabetic milieu, while KC and G-CSF paralleled their protein response. Further, mouse MIP-1α was also strongly upregulated at the mRNA level (Figure 5).

We also tested the hypothesis that chemokine KC and G-CSF may exert direct effects on islet function. Both factors were initially tested at 1-100 ng/mL, with maximal effects seen at 100 ng/mL. When added at 100 ng/ml for 4 days, both factors had a mild effect on β-cell apoptosis [control: 0.33 $\pm$ 0.11; 100 ng/ml KC: 0.85 $\pm$ 0.35; 100 ng/ml G-CSF: 0.41 $\pm$ 0.03 TUNEL β-cells/islet ($p>0.05$, n=5), with a minimal effect on glucose-stimulated insulin secretion (control: 2.9 $\pm$ 0.2 fold; 100 ng/ml KC: 2.3 $\pm$ 0.3 fold insulin secretion ($p<0.05$, n=4)]. Thus, we hypothesized that these factors were more important in mediating indirect effects on islets rather than having direct effects on β-cells themselves.

To evaluate whether *in vitro* regulation of cytokine/chemokine release by a diabetic milieu could be relevant *in vivo*, C57BL/6J mice were subjected to HF diet feeding in order to investigate the islets *ex vivo*. After 4 weeks on HF diet there was no increase in *ex vivo* islet cytokine/chemokine release despite a slight impairment in islet function as assessed by glucose-stimulated insulin secretion (not shown). However, after 8 weeks of HF feeding there was both an impairment in islet function, and a doubling of the same cytokines/chemokines regulated by a diabetic milieu *in vitro* (IL-6, chemokine KC, and G-CSF) compared to control islets (Figure 6). Finally, circulating serum KC was significantly elevated in 8 week HF fed animals versus controls (Figure 6B, $p<0.05$, n=4). The present study and independent experiments in our laboratory have found no increase in islet area by 8 weeks of high fat feeding (data not shown; n=5), indicating that these effects are not secondary to an increase in islet mass.

IL-8 co-localizes to human α-cells, and mediates the migration of monocytes and neutrophils towards isolated islets exposed to a type 2 diabetic milieu. Given those factors induced by a type 2 diabetic milieu in human islets, we hypothesized that the chemokine IL-8 may be responsible for the migration of monocytes towards islets in type 2 diabetes. IL-8 is known to attract both monocytes and neutrophils, and it was most strongly induced by glucolipotoxicty in human islets (Figure 3D). Initially, we analyzed the localization of IL-8 in the human pancreas and in human isolated islets. We found IL-8 expression in human islets to be localized to glucagon-positive endocrine cells, suggesting that islet IL-8 is mainly α-cell-derived (Figure 7A; 1-15). Indeed, by EM on ultrathin serial sections of isolated human islets, IL-8 was co-localized to glucagon-positive α-cell granules

(Figure 7B) and not found in β-cells or δ-cells (not shown). The specificity of the antibody used for immunostaining was isotype controlled, tested by preabsorption with recombinant IL-8, tested on a positive control tissue (Figure 7A), and confirmed to bind the 8 kD IL-8 protein in isolated human islets by Western blot (Figure 7C).

Next, we tested the hypothesis that those factors released by pancreatic islets exposed to a type 2 diabetic milieu may recruit leukocytes. Flow cytometry analysis of migrated leukocytes revealed that conditioned medium taken from human islets had no effect on T-cell, B-cell, and NK cell migration (data not shown). However, monocyte and neutrophil migration was clearly increased by conditioned medium taken from diabetic milieu treated human islets (from islets treated with 33 mM glucose and 0.5 mM pamitate; "treated") compared to conditioned medium from untreated human islets ("untreated"; Figure 7D). Intriguingly, IL-8 neutralization completely reversed the increased monocyte and neutrophil migration induced by treatment of human islets with a diabetic milieu (Figure 7D). When taken together with the human and mouse islet *in vitro* and *ex vivo* data, this supports the concept that IL-8 (or possibly chemokine KC in the rodent) may contribute to the immune cell infiltration we have observed in type 2 diabetes.

DISCUSSION

To the best of our knowledge, macrophage infiltration of pancreatic islets has not been systematically investigated in type 2 diabetes. Our data support the conclusion that increased numbers of immune cells, specifically macrophages, are associated with pancreatic islets in type 2 diabetes. Further, increased numbers of immune cells were associated with islets of type 2 diabetes models, including the high fat fed C57BL/6J mouse, the GK rat, and the diabetic db/db mouse. Given the accumulation of immune cells around and within type 2 diabetic islets and our *in vitro* data highlighting the specificity of this response to endocrine cells, it is probable that this inflammatory process is directed towards the endocrine pancreas. This is keeping in mind that in obese patients other organs may display typical inflammatory characteristics; e.g. macrophages in adipose tissue (2; 3) and in atherosclerotic plaques (25).

Whether the presence of macrophages is causative to type 2 diabetes islet pathology requires further investigation. Hess and colleagues have shown that bone marrow cells home to damaged β-cells in a peri-islet fashion to promote islet regeneration (26). Possibly, early infiltration of macrophages may be beneficial to islet function and plasticity. However, as the disease progresses macrophages may play a role in accelerating pancreatic islet-cell dysfunction and death. The presence of macrophages may also occur post-β-cell demise, acting to phagocytose dead islet tissue. To this end, we did not detect apoptotic cells in the vicinity of infiltrating immune cells.

To further explore the molecular signals underlying increased numbers of macrophages associated with type 2 diabetic islets

we investigated the release of cytokines and chemokines from both human and mouse islets exposed to a type 2 diabetic milieu and *ex vivo* from HF fed animals. In all cases we saw a pronounced increase in IL-6, IL-8, chemokine KC (rodent islets only), G-CSF, and MIP-1α (human islets only) release due to a type 2 diabetic milieu. Further, in mouse islets, the increased release of KC and G-CSF could be blunted by treatment of islets with IL-1Ra, the endogenous receptor antagonist of IL-1β ($n=10$, $p<0.05$, J.A. Ehses and M.Y. Donath, unpublished data). This suggests that β-cell production of IL-1β in diabetic islets (27; 28) may be a key regulator of the increased chemokine production. Furthermore, IL-1β, or other effector mechanisms, may be at the origin of the observed increased rate of β-cell apoptosis, since the macrophages were not associated with apoptotic cells. Therefore, antagonism of IL-1 in patients with type 2 diabetes may protect the islets not only from the direct toxic effects of IL-1β but also from the consecutive inflammatory process (29).

While further investigation is required to test the true cellular origin of islet derived chemokines both *in vitro* and *in vivo*, our data suggest they are pancreatic islet cell-derived. This may include an endocrine, endothelial, neuronal, and/or resident macrophage (or other immune cells) origin. However, in contrast to IL-8, G-CSF and MIP-1α, nutrient regulation of IL-6 seems not to occur at the mRNA level in islets, and its production level is similar in islets and non-islet pancreatic tissue. Our data is supported by a preliminary report that elevated palmitate can upregulate chemokine KC mRNA in addition to other chemokines (MCP-1, SDF-1) in MIN-6 β-cells (30). In addition, transcripts for chemokines in isolated β-cells and β-cell lines have been shown to be induced by cytokines mimicking the type 1 diabetic milieu (IL-1β, TNFα, IFNγ) (31-34). Chemokine KC was also strongly induced in these studies (33; 34). Comparing these studies with our data shows that both the pattern of islet chemokines induced by glucose/palmitate versus IL-1β (or a cytokine cocktail) as well as the magnitude of effect, may be different. However, these differences may simply be due to concentration-dependent effects of IL-1β.

Increased migration of both monocytes and neutrophils was induced by conditioned medium from islets exposed to a type 2 diabetic milieu, and was completely reversed by IL-8 neutralization. Thus, IL-8 presents itself as an intriguing candidate contributing to inflammation in type 2 diabetic islets. Circulating IL-8 has been shown to be elevated in type 2 diabetics (10; 11), and IL-8 expression is elevated in the adipose tissue of obese insulin resistance subjects (35). Further, hyperglycemia has been shown to increase aortic endothelial cell IL-8 secretion and thereby promote monocyte adhesion (13). Our levels of IL-8 release are very similar to those needed for monocyte adhesion to endothelia (12; 13). Given that circulating IL-8 levels are very low, it is possible that islet produced IL-8 may promote a concentration gradient leading to monocyte transmigration and infiltration.

In conclusion, we have detected the presence of increased numbers of macrophages in pancreatic islets from patients with type 2 diabetes. In fact, in HF fed mice and GK rats increased islet macrophages were detected early during disease progression. Furthermore, elevated glucose and palmitate concentrations increased chemokine release from human and mouse pancreatic islets both *in vitro* and *ex vivo*. In particular, we localized IL-8 to the human α-cell and demonstrated the ability of a type 2 diabetic milieu to enhance immune cell chemotaxis, an effect regulated by islet-derived IL-8.

ACKNOWLEDGEMENTS

We thank M. Borsig, I. Danneman, G. Seigfried-Kellenberger, E. Katz, and J. Coulaud for excellent technical assistance, and W. Moritz for technical advice regarding immunohistochemistry. This work was supported by grants from the Swiss National Science Foundation grant # PP00B-68874/1, the European Foundation for the Study of Diabetes, and the University Research Priority Program "Integrative Human Physiology" at the University of Zürich. J.A.E. is supported by a Juvenile Diabetes Research Foundation postdoctoral fellowship.

REFERENCES

1. Wellen KE, Hotamisligil GS: Inflammation, stress, and diabetes. *J Clin Invest* 115:1111-1119, 2005
2. Xu H, Barnes GT, Yang Q, Tan G, Yang D, Chou CJ, Sole J, Nichols A, Ross JS, Tartaglia LA, Chen H: Chronic inflammation in fat plays a crucial role in the development of obesity-related insulin resistance. *J Clin Invest* 112:1821-1830, 2003
3. Weisberg SP, McCann D, Desai M, Rosenbaum M, Leibel RL, Ferrente Jr. AW: Obesity is associated with macrophage accumulation in adipose tissue. *J Clin Invest* 112:1796-1808, 2003
4. Arkan MC, Hevener AL, Greten FR, Maeda S, Li ZW, Long JM, Wynshaw-Boris A, Poli G, Olefsky J, Karin M: IKK-beta links inflammation to obesity-induced insulin resistance. *Nat Med* 11:191-198, 2005
5. Kolb H, Mandrup-Poulsen T: An immune origin of type 2 diabetes? *Diabetologia* 48:1038-1050, 2005
6. Hoffmann E, Dittrich-Breiholz O, Holtmann H, Kracht M: Multiple control of interleukin-8 gene expression. *J Leukoc Biol* 72:847-855, 2002
7. Gerszten RE, Garcia-Zepeda EA, Lim Y-C, Yoshida M, Ding HA, Gimbrone Jr. MA, Luster AD, Luscinskas FW, Rosenzweig A: MCP-1 and IL-8 trigger firm adhesion of monocytes to vascular endothelium under flow conditions. *Nature* 398:718-723, 1999
8. Boisvert WA, Santiago R, Curtiss LK, Terkeltaub RA: A leukocyte homologue of the IL-8 receptor CXCR-2 mediates the accumulation of macrophages in atherosclerotic lesions of LDL receptor-deficient mice. *J Clin Invest* 101:353-363, 1998
9. Huo Y, Weber C, Forlow SB, Sperandio M, Thatte J, Mack M, Jung S, Littman DR, Ley K: The chemokine KC, but not monocyte chemoattractant protein-1, triggers monocyte arrest on early atherosclerotic endothelium. *J Clin Invest* 108:1307-1314, 2001
10. Esposito K, Nappo F, Giugliano F, Di Palo C, Ciotola M, Barbieri M, Paolisso G, Giugliano D: Cytokine mileau tends toward inflammation in Type 2 diabetes. *Diabetes Care* 26:1647, 2003
11. Zozulinska D, Majchrzak A, Sobieska K, Wiktorowicz K, Wierusz-Wysocka B: Serum interleukin-8 level is increased in diabetic patients. *Diabetologia* 42:117-118, 1999
12. Srinivasan S, Bolick DT, Hatley ME, Natarajan R, Reilly KB, Yeh M, Chrestensen C, Sturgill TW, Hedrick CC: Glucose regulates interleukin-8 production in aortic endothelial cells through activation of the p38 mitogen-activated protein kinase pathway in diabetes. *J Biol Chem* 279:31930-31936, 2004
13. Srinivasan S, Yeh M, Danziger EC, Hatley ME, Riggan AE, Leitinger N, Berliner JA, Hedrick CC: Glucose regulates monocyte adhesion through endothelial production of interleukin-8. *Circ Res* 92:371-377, 2003
14. Lampe JB, Schneider-Schaulies S, Aguzzi A: Expression of the interferon-induced MxA protein in viral encephalitis. *Neuropathol Appl Neurobiol* 29:273-279, 2003
15. Lalive PH, Paglinawan R, Biollaz G, Kappos EA, Leone DP, Malipiero U, Relvas JB, Moransard M, Suter T, Fontana A: TGF-beta-treated microglia induce oligodendrocyte precursor cell chemotaxis through the HGF-c-Met pathway. *Eur J Immunol* 35:727-737, 2005
16. Homo-Delarche F, Calderari S, Irminger JC, Gangnerau MN, Coulaud J, Rickenbach K, Dolz M, Halban P, Portha B, Serradas P: Islet Inflammation and Fibrosis in a Spontaneous Model of Type 2 Diabetes, the GK Rat. *Diabetes* 55:1625-1633, 2006
17. Desbaillets I, Diserens A-C, de Tribolet N, Hamou M-F, Van Meir EG: Upregulation of interleukin-8 by oxygen-deprived cells in glioblastoma suggests a role in leukocyte activation, chemotaxis, and angiogenesis *J Exp Med* 186:1201-1212, 1997
18. Portha B, Giroix MH, Serradas P, Gangnerau MN, Movassat J, Rajas F, Bailbe D, Plachot C, Mithieux G, Marie JC: Beta-cell function and viability in the spontaneously diabetic GK rat: information from the GK/Par colony. *Diabetes* 50 Suppl 1:S89-93, 2001
19. Gmyr V, Belaich S, Muharram G, Lukowiak B, Vandewalle B, Pattou F, Kerr-Conte J: Rapid purification of human ductal cells from human pancreatic fractions with surface antibody CA19-9. *Biochem Biophys Res Commun* 320:27-33, 2004

20. Ichii H, Inverardi L, Pileggi A, Molano RD, Cabrera O, Caicedo A, Messinger S, Kuroda Y, Berggren PO, Ricordi C: A novel method for the assessment of cellular composition and beta-cell viability in human islet preparations. *Am J Transplant* 5:1635-1645, 2005
21. Minami K, Okuno M, Miyawaki K, Okumachi A, Ishizaki K, Oyama K, Kawaguchi M, Ishizuka N, Iwanaga T, Seino S: Lineage tracing and characterization of insulin-secreting cells generated from adult pancreatic acinar cells. *Proc Natl Acad Sci U S A* 102:15116-15121, 2005
22. Maedler K, Sergeev P, Ehses JA, Mathe Z, Bosco D, Berney T, Dayer JM, Reinecke M, Halban PA, Donath MY: Leptin modulates beta-cell expression of the IL-1 receptor antagonist and release of IL-1beta in human islets. *Proc Nat Acad Sci USA* 101:8138-8143, 2004
23. Ehses JA, Pelech SL, Pederson RA, McIntosh CH: Glucose-dependent insulinotropic polypeptide (GIP) activates the Raf-Mek 1/2-ERK 1/2 module via a cyclic AMP/PKA/Rap1-mediated pathway. *J Biol Chem* 277:37088-37097, 2002
24. Cancello R, Henegar C, Viguerie N, Taleb S, Poitou C, Rouault C, Coupaye M, Pelloux V, Hugol D, Bouillot JL, Bouloumie A, Barbatelli G, Cinti S, Svensson PA, Barsh GS, Zucker JD, Basdevant A, Langin D, Clement K: Reduction of macrophage infiltration and chemoattractant gene expression changes in white adipose tissue of morbidly obese subjects after surgery-induced weight loss. *Diabetes* 54:2277-2286, 2005
25. Rader DJ, Puré E: Lipoproteins, macrophage function, and atherosclerosis: Beyond the foam cell? *Cell Metab* 1:223-230, 2005
26. Hess D, Li L, Martin M, Sakano S, Hill D, Strutt B, Thyssen S, Gray DA, Bhatia M: Bone marrow-derived stem cells initiate pancreatic regeneration. *Nat Biotechnol* 21:763-770, 2003
27. Maedler K, Sergeev P, Ris F, Oberholzer J, Joller-Jemelka HI, Spinas GA, Kaiser N, Halban PA, Donath MY: Glucose-induced beta cell production of IL-1beta contributes to glucotoxicity in human pancreatic islets. *J Clin Invest* 110:851-860, 2002
28. Boeni-Schnetzler M, Marselli L, Ehses JA, Marchetti P, Weir GC, Donath MY: IL-1beta expression is induced by glucose and IL-1beta auto-stimulation, and increased in beta cells of type 2 diabetics. *Diabetes* Suppl, 2007
29. Larsen CM, Faulenbach M, Vaag A, Volund A, Ehses JA, Seifert B, Mandrup-Poulsen T, Donath MY: Interleukin-1-receptor antagonist in type 2 diabetes mellitus. *N Engl J Med* 356:1517-1526, 2007
30. Busch AK, Cordery D, Denyer GS, Biden TJ: Expression profiling of palmitate-and oleate-regulated genes provides novel insights into the effects of chronic lipid exposure on pancreatic beta-cell function. *Diabetes* 51:977-987, 2002
31. Arnush M, Heitmeier MR, Scarim AL, Marino MH, Manning PT, Corbett JA: IL-1 produced and released endogenously within human islets inhibits beta cell function. *J Clin Invest* 102:516-526, 1998
32. Frigerio S, Junt T, Lu B, Gerard C, Zumsteg U, Hollander GA, Piali L: Beta-cells are responsible for CXCR3-mediated T-cell infiltration in insulitis. *Nature Med* 8:1414-1420, 2002
33. Chen MC, Schuit F, Eizirick DL: Identification of IL-1beta-induced messenger RNAs in rat pancreatic beta cells by differential display of messenger RNA. *Diabetologia* 42:1199-1203, 1999
34. Rasschaert J, Liu D, Kutlu B, Cardozo AK, Kruhoffer M, ORntoft TF, Eizirick DL: Global profiling of double stranded RNA- and IFN-gamma-induced genes in rat pancreatic beta cells. *Diabetologia* 46:1641-1657, 2003
35. Rotter V, Nagaev I, Smith U: Interleukin-6 (IL-6) induces insulin resistance in 3T3-L1 adipocytes and is, like IL-8 and tumor necrosis factor-alpha, overexpressed in human fat cells from insulin-resistant subjects. *J Biol Chem* 278:45777-45784, 2003

Table 1: **Source of tissue samples used for analysis of CD68, CD163, CD3, and HLA-2 in diabetic and non-diabetic individuals.** All tissue samples were obtained from the Department of Pathology, University Hospital of Zurich, Switzerland. Patients with pancreatitis, lymphoma, systemic infection, and on immunosuppressive therapy were excluded from analysis.

	Patient no.	Age (yrs)	Sex (M/F)	BMI (kg/m2)	FPG (mM)	Source of pancreas	Reason	Diabetes therapy
Nondiabetic	1	51	M	21	4.7	Operation	Carcinoma	N/A
	2	63	F	N/A	4	Operation	Benign endocrine pancreas tumor	N/A
	3	63	M	23	4.4	Operation	Carcinoma	N/A
	4	89	F	25	3.6	Necropsy	Aorta dissection	N/A
	5	81	F	25	5.3	Necropsy	Ischemic heart disease	N/A
	6	74	F	24	5.7	Necropsy	Cardiac shock	N/A
	7	72	M	21	4.5	Necropsy	Ischemic heart disease	N/A
Mean		**70**		**23.2**	**4.6**			
Diabetic	8	64	M	26	11.7	Operation	Carcinoma	Diet
	9	66	F	29	7.3	Operation	Benign endocrine pancreas tumor	Insulin
	10	63	F	33	15	Operation	Carcinoma	Diet
	11	68	M	32	10.7	Operation	Ectopic spleen, normal pancreas	Diet
	12	61	M	N/A	16	Organ Donor	Transplantation	N/A
	13	83	F	23	9.8	Necropsy	Ischemic heart disease	Diet
	14	77	M	26	8.4	Necropsy	Ventricular fibrillation	Oral antidiabetic (metformin)
	15	56	F	22	25	Necropsy	Ischemic heart disease	Diet
	16	74	F	23	14.7	Necropsy	Ischemic heart disease	Oral antidiabetic (metformin)
Mean		**68**		**26.8 ***	**13.2 ***			

* $p<0.05$ vs nondiabetic patients. N/A = not available/not applicable

FIGURE LEGENDS

Figure 1. **Increased number of islet macrophages in type 2 diabetic islets.** Increased islet associated macrophages in human type 2 diabetic islets (A-B) and the high fat fed C57BL/6J mouse (C-E). In (A-B), islet-associated macrophages were detected by insulin (red) and CD68 (brown, arrows) staining of organ samples (see Table 1 for tissue sources). A representative control islet (B, 1), an islet from a type 2 diabetic patient (B, 2), and an isotype control stained islet (B, 3) are shown. In serial sections, TUNEL+ cells were evaluated in CD68+ infiltrated human islets and a representative islet from a type 2 diabetic patient stained for CD68 (B, 4) and TUNEL (B, 5) is shown. The CD68+ region outlined in (B, 4) is enlarged in (B, 6). All images are 200X, except (B, 6) which is shown at 400X. Islet associated Cd11b+ cells (C) were increased around large islets in 8 and 16 week HF fed C57BL/6J animals versus equal-sized normal chow control islets (n=3-7). IPGTTs are shown for each group of animals (C). In (D-E), islet-associated Cd11b+ cells (7 and 8) and antibody specificity (9 and 10) are shown in C57BL/6J mice (8 week chow and HF fed). All images are 200X. Where * represents $p<0.05$ as determined using Student's t-test.

Figure 2. **Increased number of islet macrophages in the GK rat.** Increased islet associated macrophages were detected in the 2-month old GK rat. Macrophages were stained using anti-CD68 (brown; E) and anti-MHC class 2 antibodies with H & E counterstaining. Numbers of islet associated CD68 (A) and MHC-2 cells (C) were scored in 6 to 9 different animals. The mean islet area was identical in both strains for these comparisons (B and D). Representative images of a control Wistar islet (E, 1) and a GK islet (E, 2) stained for CD68 (arrows) are shown. Where * represents $p<0.05$ as determined using Student's t-test.

Figure 3. **Elevated glucose and palmitate increase cytokine/chemokine release from mouse and human islets.** It was confirmed that 48 h treatment with 33 mM glucose (33 mM) and 0.5 mM palmitate (16:0; alone or in combination) were detrimental to mouse and human islet function (A, B). Islet function (A) was assessed by acute (1 h) glucose stimulated insulin secretion (mouse n=3-6; human n=7). Simultaneously, after 48 h of treatment with 33 mM glucose and 0.5 mM palmitate (alone or in combination) cytokines/chemokines were assayed (C-H) from mouse and human islet conditioned medium representing 20 islets/dish. Basal concentrations of cytokines/chemokines for human islet experiments are provided on respective graphs. All experiments were conducted in triplicate (mouse n=3-6; human n=7), where * represents $p<0.05$ as tested by Student's t-test, or ANOVA with Dunnett's post hoc test.

Figure 4. **Specificity of the inflammatory response to elevated glucose and palmitate in islets, non-endocrine tissue, and β-cell lines.** Mouse pancreatic islets and non-endocrine pancreatic tissue were plated on ECM dishes and treated for 48 h with 33 mM glucose and 0.5 mM palmitate (33/16:0). Conditioned medium was assayed for IL-6 (A), chemokine KC (B), G-CSF (C), and IP-10 (D)

and corrected for total protein. MIN-6 cells and INS-1 cells were plated in 24-well plates and treated for 48 h with 33 mM glucose (33 mM) and 0.5 mM palmitate (16:0; alone or in combination). Conditioned medium was assayed for chemokine KC (E, F), G-CSF (G), and MIP-1α (H) and corrected for total protein. Mouse pancreatic islets were treated for 48 h with 0.1 and 1 mM streptozotocin (I), or 500 nM staurosporine (J). Conditioned medium was assayed for detection of IL-6, chemokine KC, and G-CSF. Streptozotocin (1 mM) and staurosporine (500 nM) were confirmed to induce cell death by TUNEL staining (K). Conditioned medium was always collected at the end of the 48 h treatment period. All experiments were conducted in triplicate (A-D: n=4; E: n=2; F-H: n=5; I-K: n=3), where * and # represent $p<0.05$ as determined using ANOVA with Bonferonni's post hoc test.

Figure 5. **Elevated glucose and palmitate increase chemokine KC, G-CSF, and MIP-1α mRNA in mouse islets.** Mouse islets were isolated and treated with 33 mM glucose (33 mM) and 0.5 mM palmitate (16:0; alone or in combination) for 48 h. Total islet RNA was extracted and reverse transcribed using random hexamers. Primers were used to detect IL-6 (A), chemokine KC (B), G-CSF (C), and MIP-1α (D) mRNA. Cytokine/chemokine mRNA vs. an 18S control was assayed using the Taqman® quantitative PCR system and data are shown as fold of control. Where * represents $p<0.05$ as tested by ANOVA and Dunnett's post hoc test (n=3-4).

Figure 6. **High fat diet increases IL-6, chemokine KC, and G-CSF release from isolated islets.** Mouse islets were isolated from animals fed normal chow or a high fat diet for 8 weeks. In (A) twenty islets/dish were plated and after 48 h assessed for islet function; HF fed animal islets showed impaired acute glucose stimulated insulin secretion vs. controls. Serum KC (B) was significantly elevated in HF fed animals after 8 weeks. Conditioned medium was assayed for IL-6 (C), chemokine KC (D), G-CSF (E), and IP-10 (F). Experiments were performed in triplicate on 5 animals (n=5), where * represents $p<0.05$ as determined using Student's t-test.

Figure 7. **IL-8 co-localizes to human α-cells, and mediates the migration of monocytes and neutrophils induced by conditioned medium from human islets.** IL-8 expression was detected in human pancreatic resection samples (A: 2, 5, 8, 11; representative of 3-7 different patient samples), isolated human non-β cells (A:14), and isolated human islets (B,C). Antibody specificity was tested by preabsorption with recombinant IL-8 (A:1-3), by isotype controls (A: 1, 5), and using brain glioblastoma as a positive control (A, 4). IL-8 staining did not co-localize with insulin positive β-cells within the pancreatic islet, and did co-localize with glucagon positive α-cells (A, 7-9; 10-12; and 13-15). Electron microscopic investigation of IL-8 and glucagon visualised with double immunogold labelling (B). Large image shows overview of a glucagon cell. N: Nucleus. Square designates region shown at higher magnification (insert). Small image reveals that some granules contain IL-8 (15 nm gold particles) and glucagon (5 nm gold

particles) immunoreactivities, whereas some are only immunoreactive for glucagon. Western blotting confirmed production of IL-8 by human islets. Shown are representative blots from two separate human islet samples, along with recombinant IL-8 as a control; the 8 kD band corresponds to IL-8 (C). Conditioned medium from the above experiment (Figure 3) was used in migration experiments with isolated human PMBCs and granulocytes (D). Human islet media was used as control; “untreated” refers to conditioned medium from untreated human islets, “treated” refers to conditioned medium from human islets treated with 33 mM glucose and 0.5 mM palmitate for 48 h. The effect of IL-8 neutralization on CD14 high expressing monocyte and CD15 high expressing neutrophil migration is shown (n=5 and n=2 respectively). Isotype IgG antibody was added to all conditions not including IL-8 Ab (“-“). Experiments were performed in triplicate, where * and # represent $p<0.05$ as determined using represent $p<0.05$ as determined using ANOVA with Bonferonni’s post hoc test.

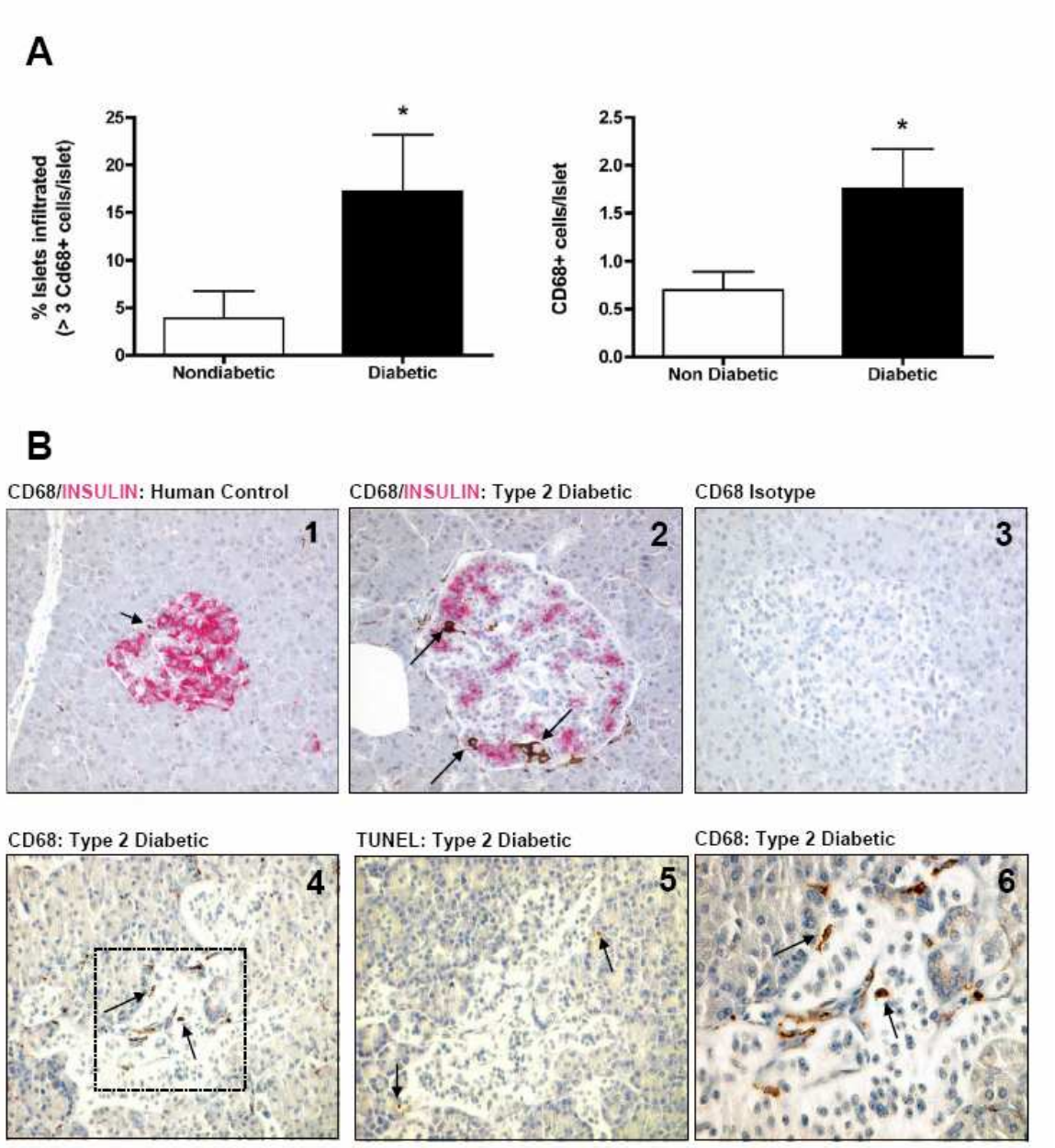
A
% Islets infiltrated (> 3 Cd68+ cells/islet)
25
20
15
10
5
0
*
Nondiabetic
Diabetic
CD68+ cells/Islet
2.5
2.0
1.5
1.0
0.5
0.0
*
Non Diabetic
Diabetic
B
CD68/INSULIN: Human Control
1
CD68/INSULIN: Type 2 Diabetic
2
CD68 Isotype
3
CD68: Type 2 Diabetic
4
TUNEL: Type 2 Diabetic
5
CD68: Type 2 Diabetic
6

Figure 1A-B

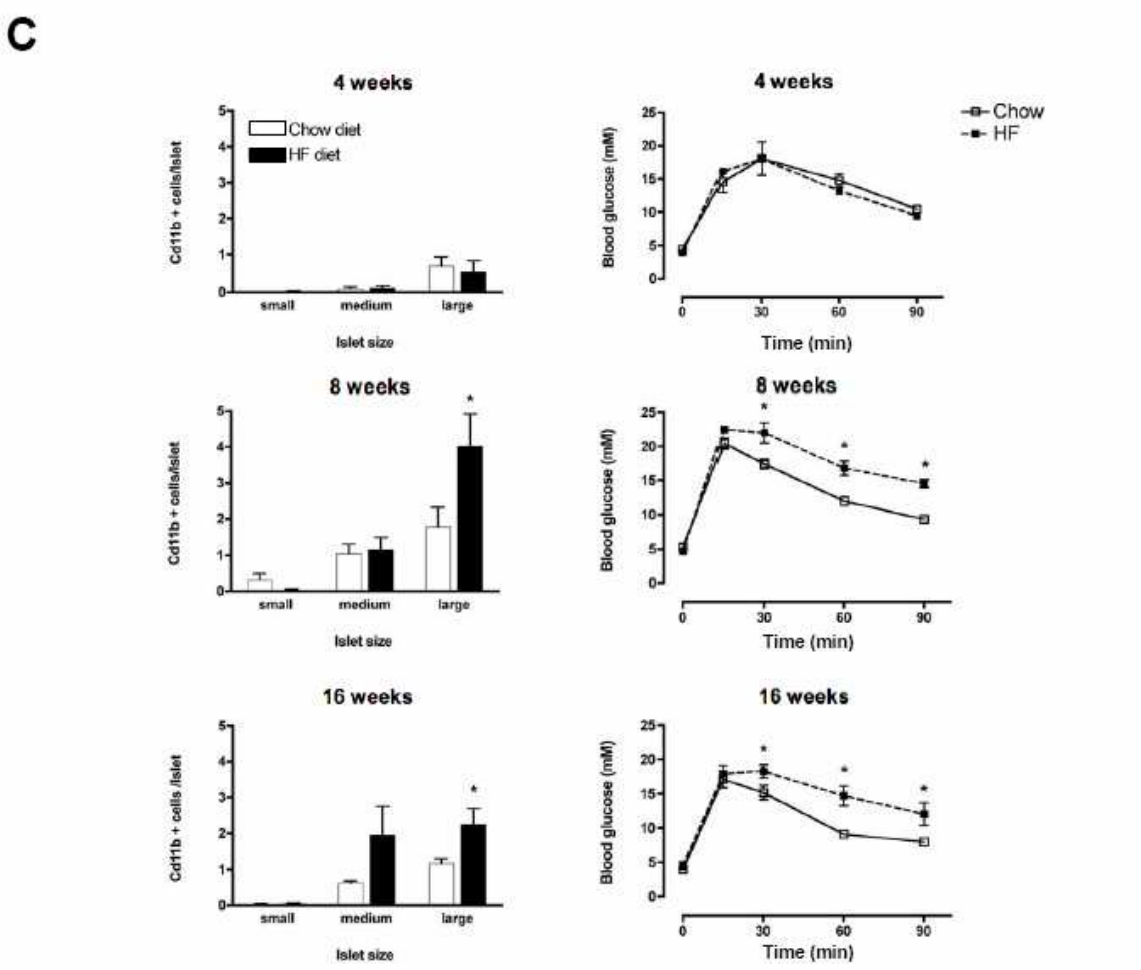
C
4 weeks
Chow diet
HF diet
Cd11b + cells/Islet
small
medium
large
Islet size
4 weeks
Chow
HF
Blood glucose (mM)
Time (min)
8 weeks
Cd11b + cells/Islet
Islet size
8 weeks
Blood glucose (mM)
Time (min)
16 weeks
Cd11b + cells /Islet
Islet size
16 weeks
Blood glucose (mM)
Time (min)

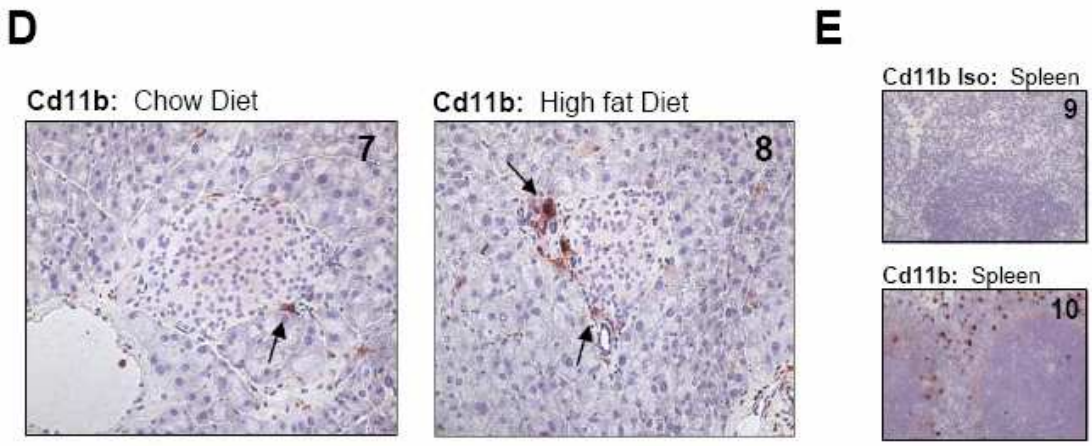
D
Cd11b: Chow Diet
7
Cd11b: High fat Diet
8
E
Cd11b Iso: Spleen
9
Cd11b: Spleen
10

Figure 1C-E

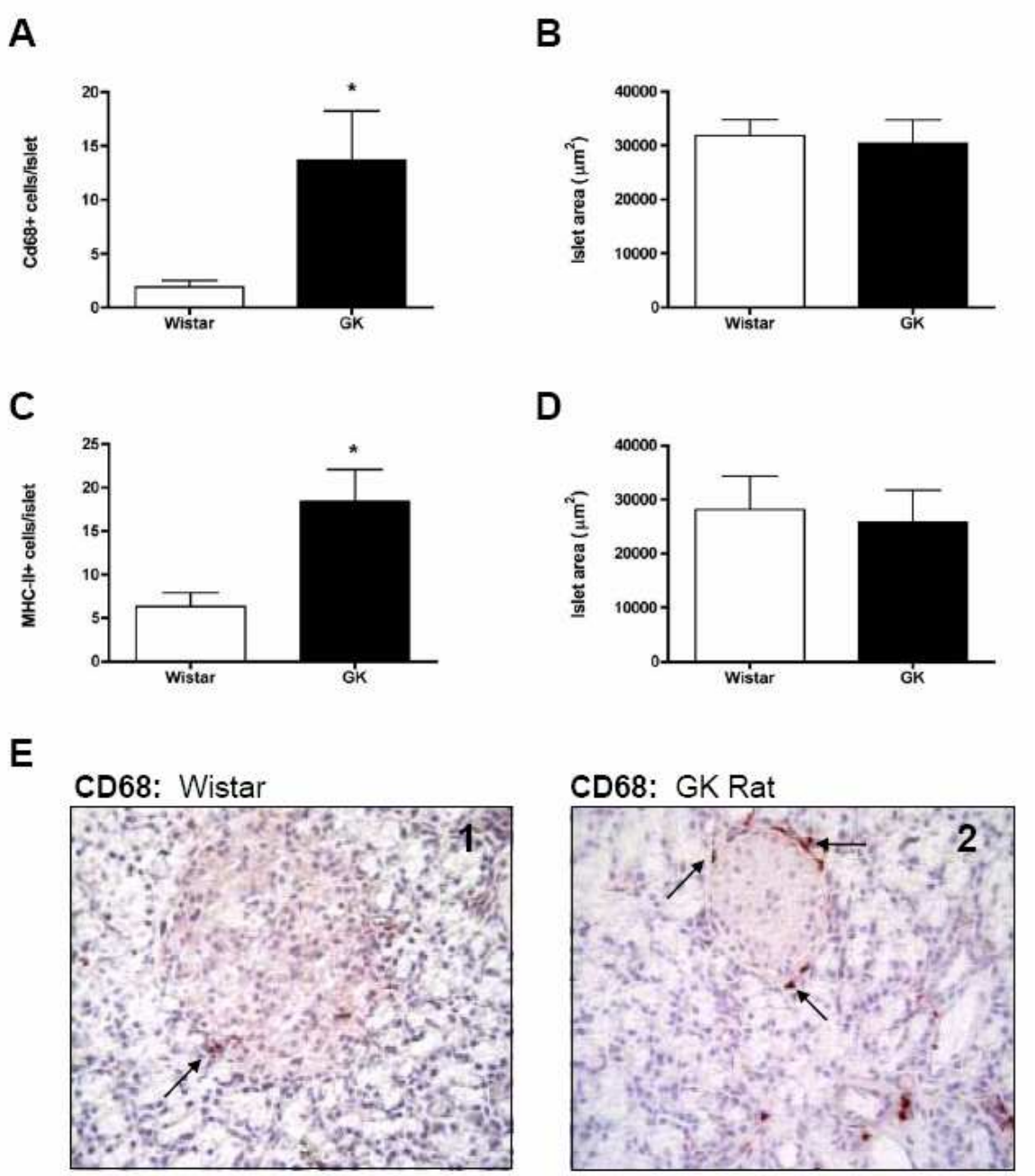
A
Cd68+ cells/islet
20
15
10
5
0
*
Wistar
GK
B
Islet area (µm²)
40000
30000
20000
10000
0
Wistar
GK
C
MHC-II+ cells/islet
25
20
15
10
5
0
*
Wistar
GK
D
Islet area (µm²)
40000
30000
20000
10000
0
Wistar
GK
E
CD68: Wistar
1
CD68: GK Rat
2

Figure 2

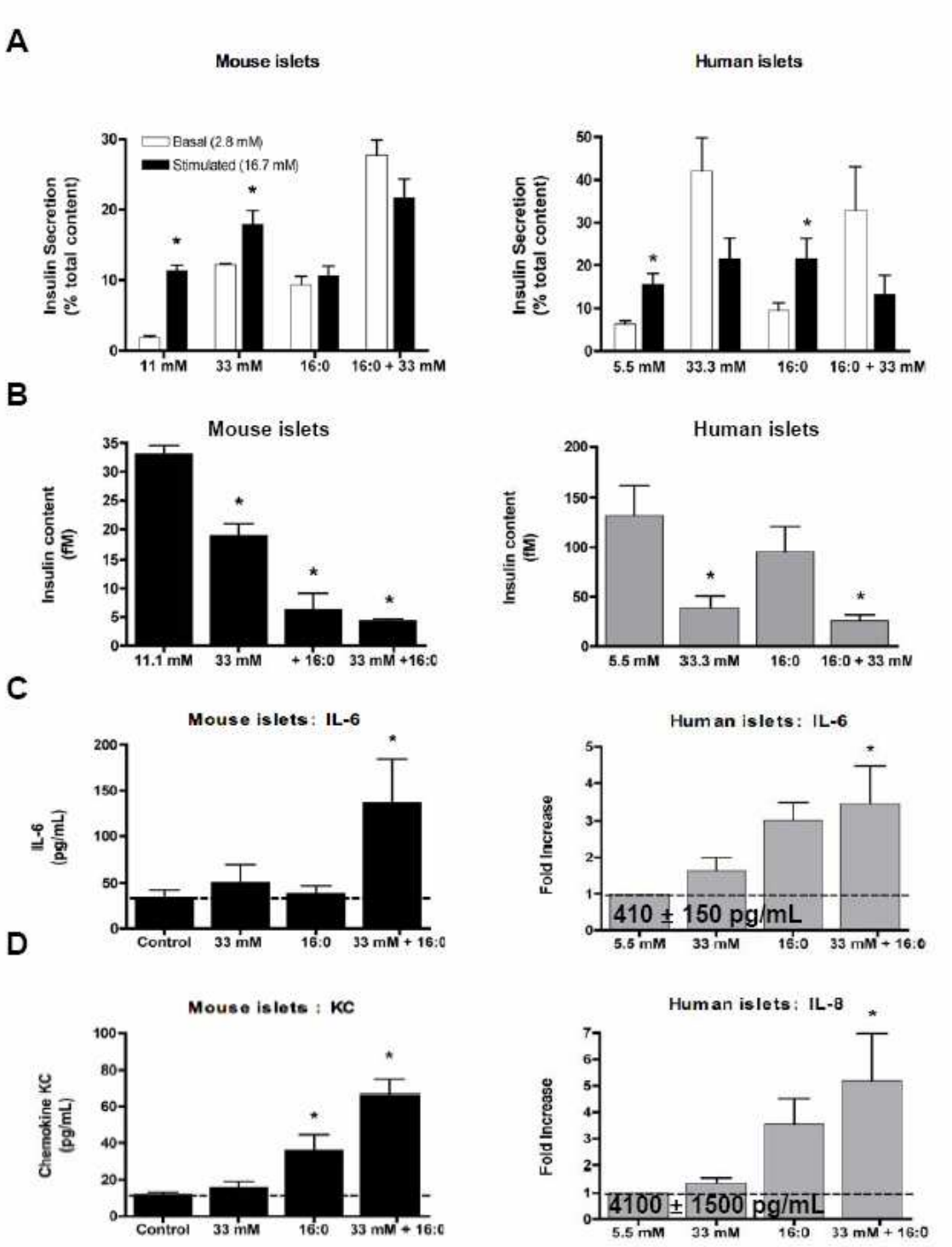
A
Mouse islets
Human islets
Basal (2.8 mM)
Stimulated (16.7 mM)
Insulin Secretion (% total content)
11 mM
33 mM
16:0
16:0 + 33 mM
5.5 mM
33.3 mM
B
Mouse islets
Human islets
Insulin content (fM)
11.1 mM
+ 16:0
33 mM +16:0
C
Mouse islets: IL-6
Human islets: IL-6
IL-6 (pg/mL)
Fold Increase
Control
410 ± 150 pg/mL
D
Mouse islets : KC
Human islets: IL-8
Chemokine KC (pg/mL)
4100 ± 1500 pg/mL

Figure 3A-D

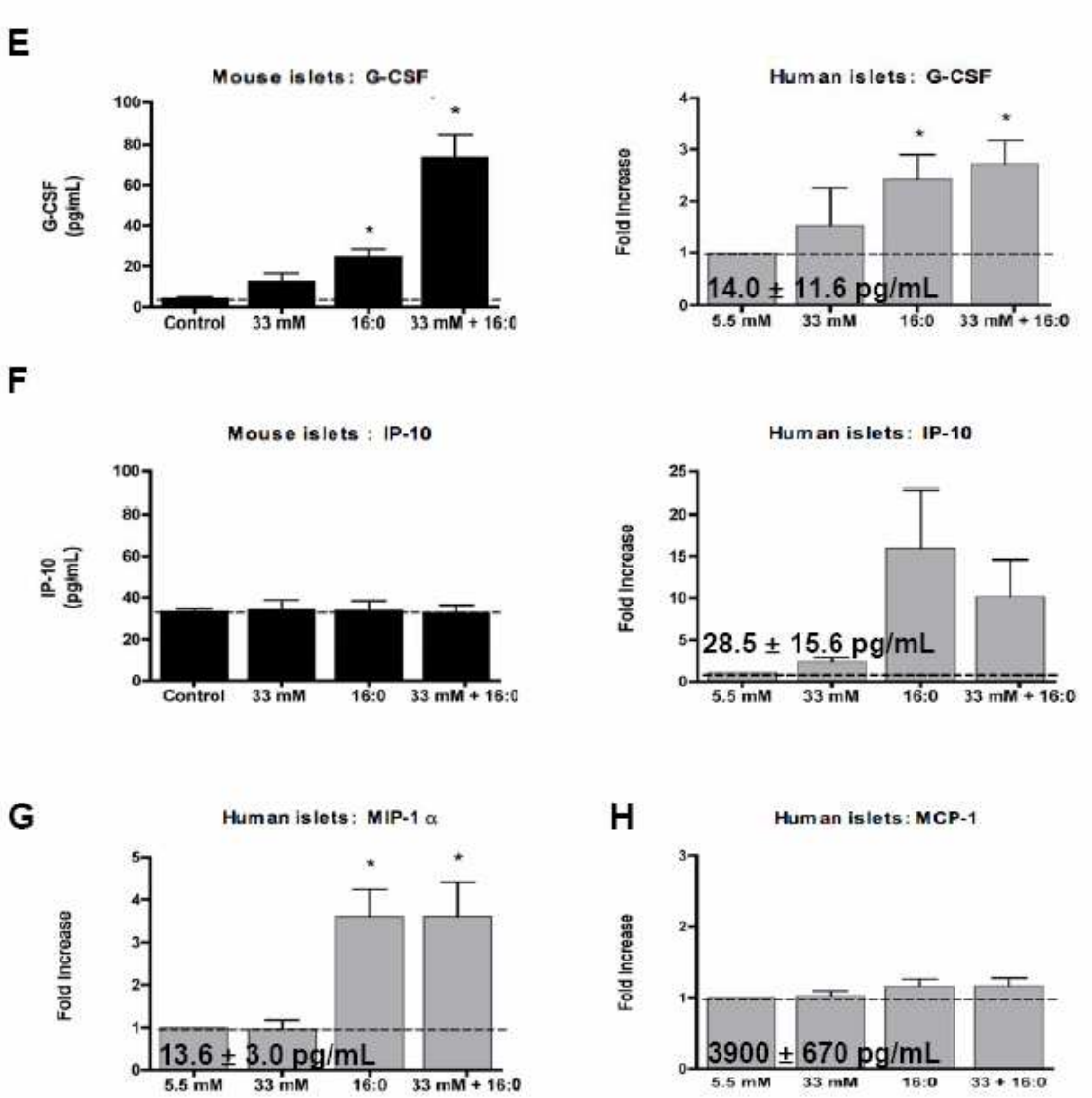
E
Mouse islets: G-CSF
G-CSF (pg/mL)
Control
33 mM
16:0
33 mM + 16:0
Human islets: G-CSF
Fold Increase
14.0 ± 11.6 pg/mL
5.5 mM
F
Mouse islets : IP-10
IP-10 (pg/mL)
Human islets: IP-10
28.5 ± 15.6 pg/mL
G
Human islets: MIP-1 α
13.6 ± 3.0 pg/mL
H
Human islets: MCP-1
3900 ± 670 pg/mL
33 + 16:0

Figure 3E-H

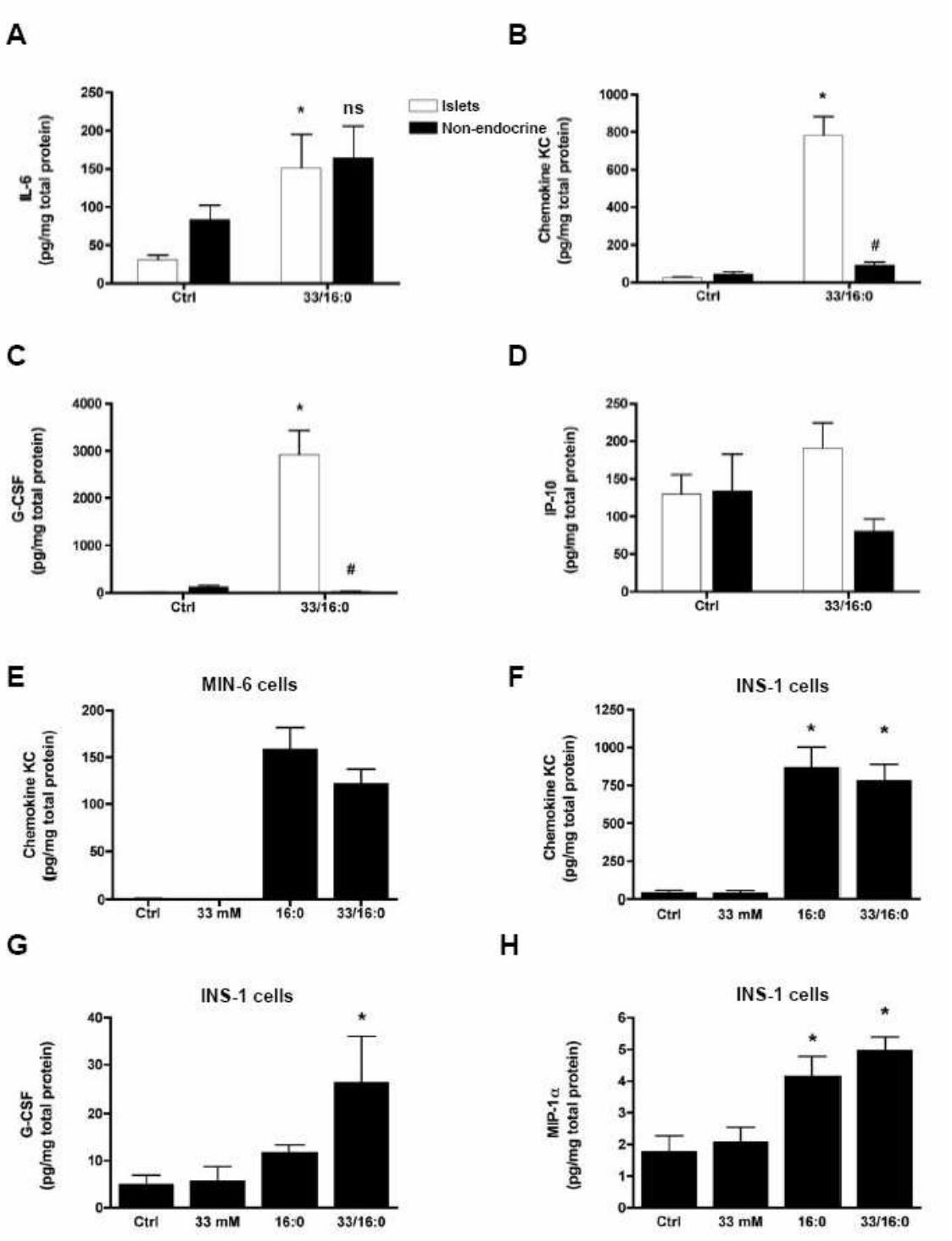
A
IL-6 (pg/mg total protein)
250
200
150
100
50
0
*
ns
Islets
Non-endocrine
Ctrl
33/16:0
B
Chemokine KC (pg/mg total protein)
1000
800
600
400
200
0
*
#
Ctrl
33/16:0
C
G-CSF (pg/mg total protein)
4000
3000
2000
1000
0
*
#
Ctrl
33/16:0
D
IP-10 (pg/mg total protein)
250
200
150
100
50
0
Ctrl
33/16:0
E
MIN-6 cells
Chemokine KC (pg/mg total protein)
200
150
100
50
0
Ctrl
33 mM
16:0
33/16:0
F
INS-1 cells
Chemokine KC (pg/mg total protein)
1250
1000
750
500
250
0
*
*
Ctrl
33 mM
16:0
33/16:0
G
INS-1 cells
G-CSF (pg/mg total protein)
40
30
20
10
0
*
Ctrl
33 mM
16:0
33/16:0
H
INS-1 cells
MIP-1α (pg/mg total protein)
6
5
4
3
2
1
0
*
*
Ctrl
33 mM
16:0
33/16:0

Figure 4A-H

Figure 4I-K

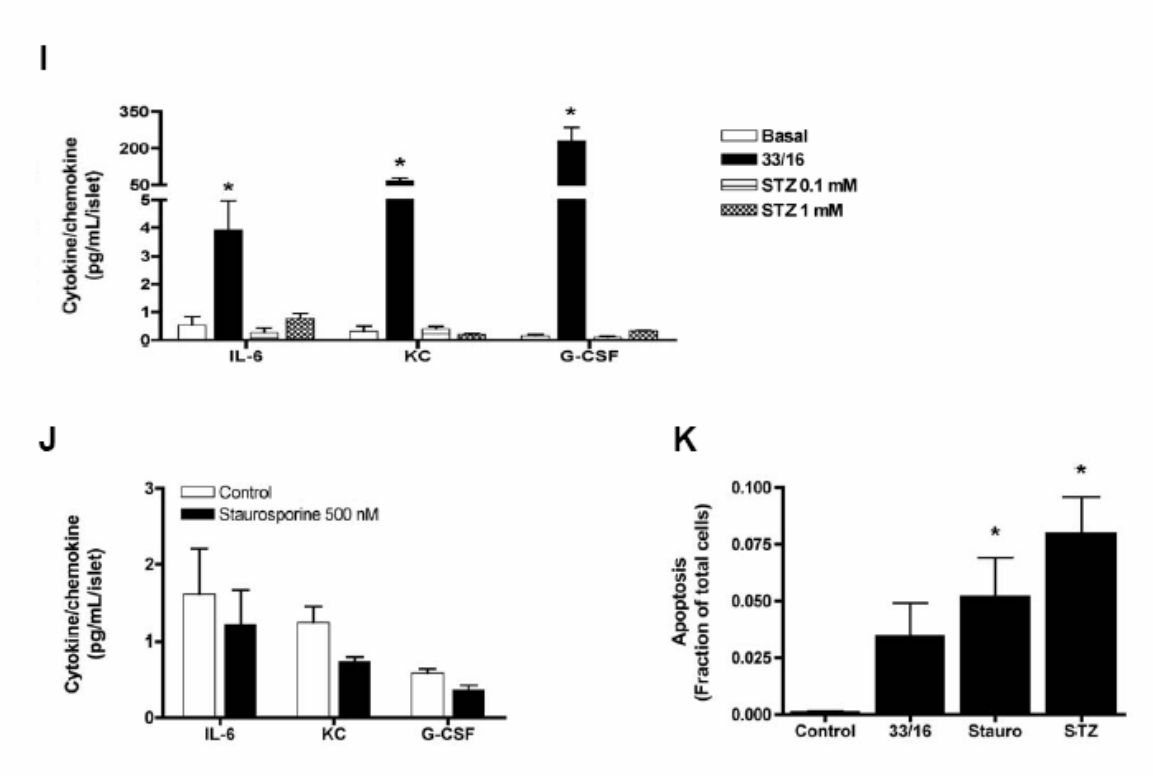
I
Cytokine/chemokine (pg/mL/islet)
350
200
50
5
4
3
2
1
0
*
*
*
IL-6
KC
G-CSF
Basal
33/16
STZ 0.1 mM
STZ 1 mM
J
Cytokine/chemokine (pg/mL/islet)
3
2
1
0
Control
Staurosporine 500 nM
IL-6
KC
G-CSF
K
Apoptosis (Fraction of total cells)
0.100
0.075
0.050
0.025
0.000
*
*
Control
33/16
Stauro
STZ

Figure 5

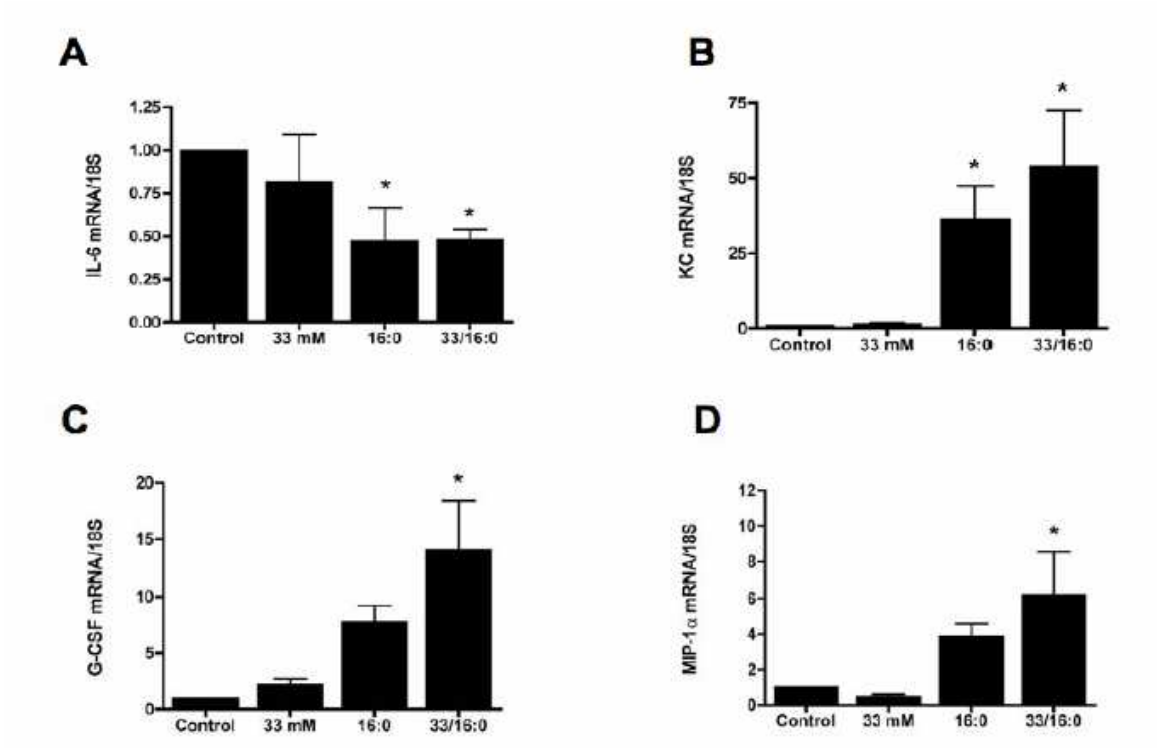
A
IL-6 mRNA/18S
1.25
1.00
0.75
0.50
0.25
0.00
Control
33 mM
16:0
33/16:0
B
KC mRNA/18S
75
50
25
0
Control
33 mM
16:0
33/16:0
C
G-CSF mRNA/18S
20
15
10
5
0
Control
33 mM
16:0
33/16:0
D
MIP-1α mRNA/18S
12
10
8
6
4
2
0
Control
33 mM
16:0
33/16:0

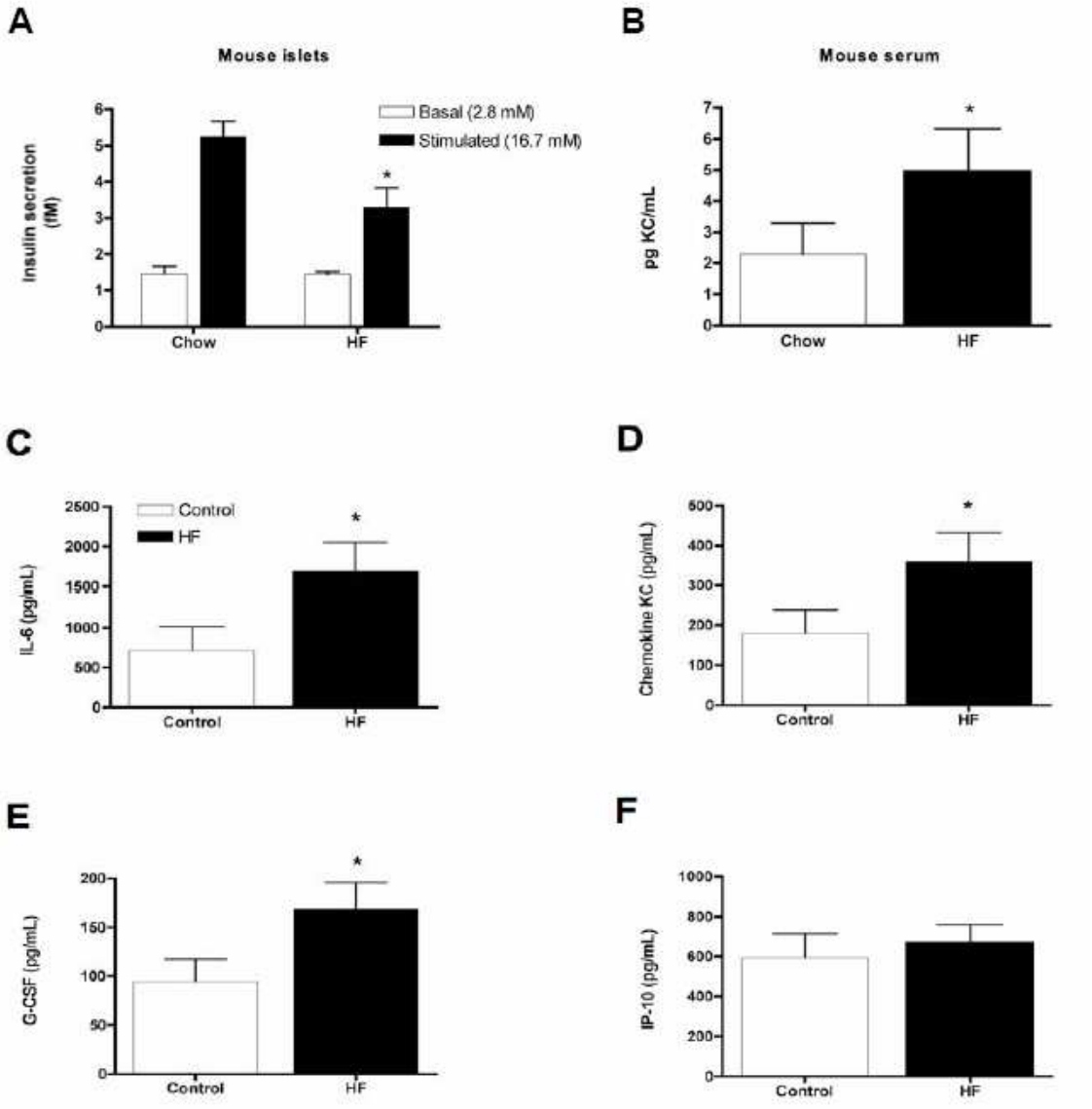
A
Mouse islets
Basal (2.8 mM)
Stimulated (16.7 mM)
Insulin secretion (fM)
Chow
HF
B
Mouse serum
pg KC/mL
Chow
HF
C
Control
HF
IL-6 (pg/mL)
Control
HF
D
Chemokine KC (pg/mL)
Control
HF
E
G-CSF (pg/mL)
Control
HF
F
IP-10 (pg/mL)
Control
HF

Figure 6

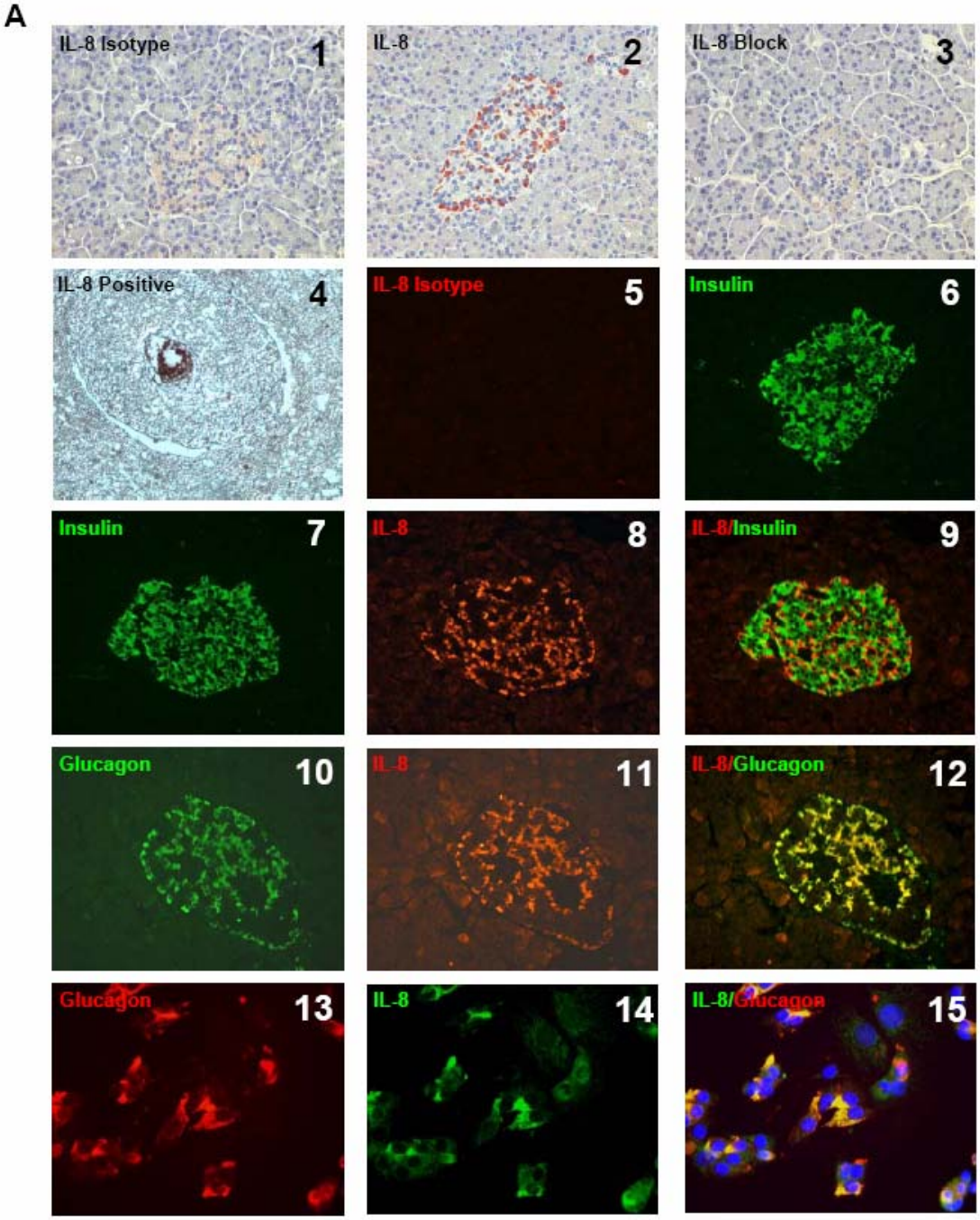
A
IL-8 Isotype
1
IL-8
2
IL-8 Block
3
IL-8 Positive
4
IL-8 Isotype
5
Insulin
6
Insulin
7
IL-8
8
IL-8/Insulin
9
Glucagon
10
IL-8
11
IL-8/Glucagon
12
Glucagon
13
IL-8
14
IL-8/Glucagon
15

Figure 7A

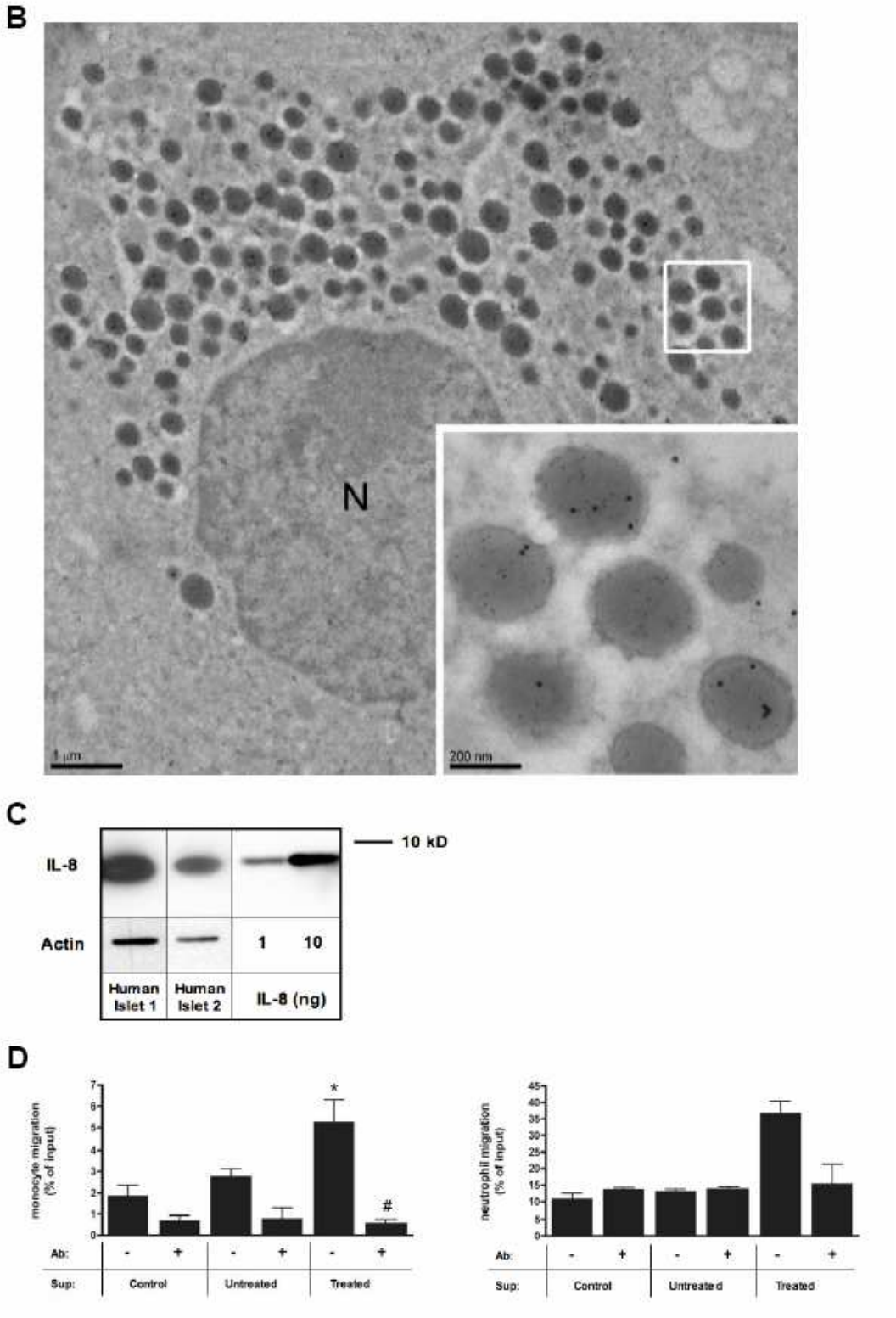
B
N
1 µm
200 nm
C
IL-8
Actin
10 kD
1
10
Human Islet 1
Human Islet 2
IL-8 (ng)
D
monocyte migration (% of input)
neutrophil migration (% of input)
Ab:
Sup:
Control
Untreated
Treated

Figure 7B-D